



School of Computing, Computational PDEs Unit

<http://www.comp.leeds.ac.uk/cpde/>

Adaptive Mesh Methods for Elastohydrodynamic Lubrication

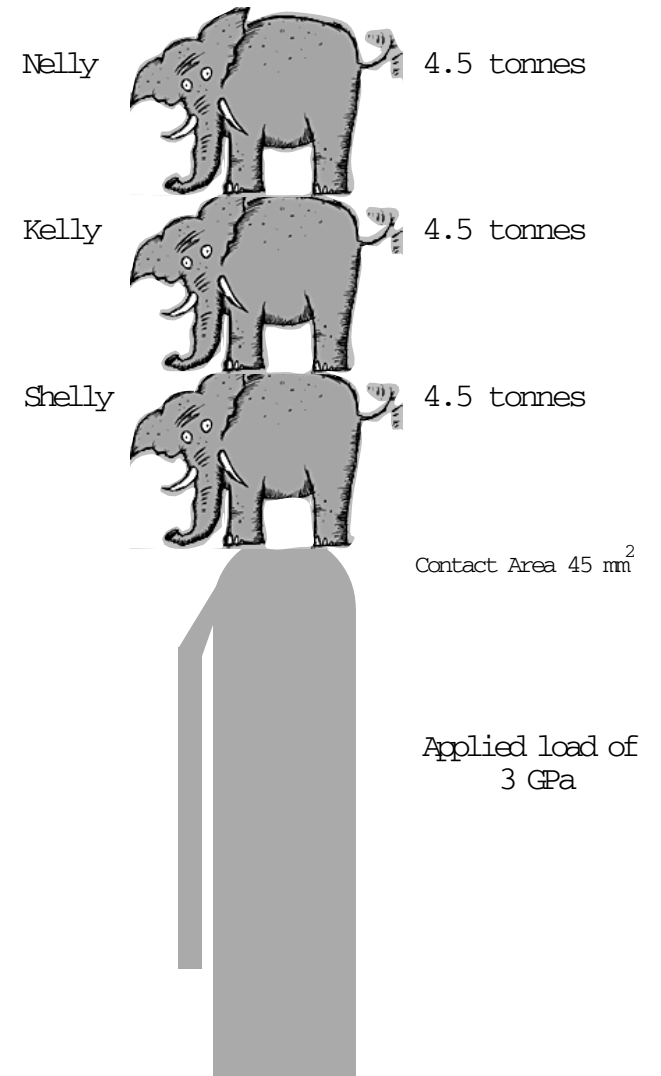
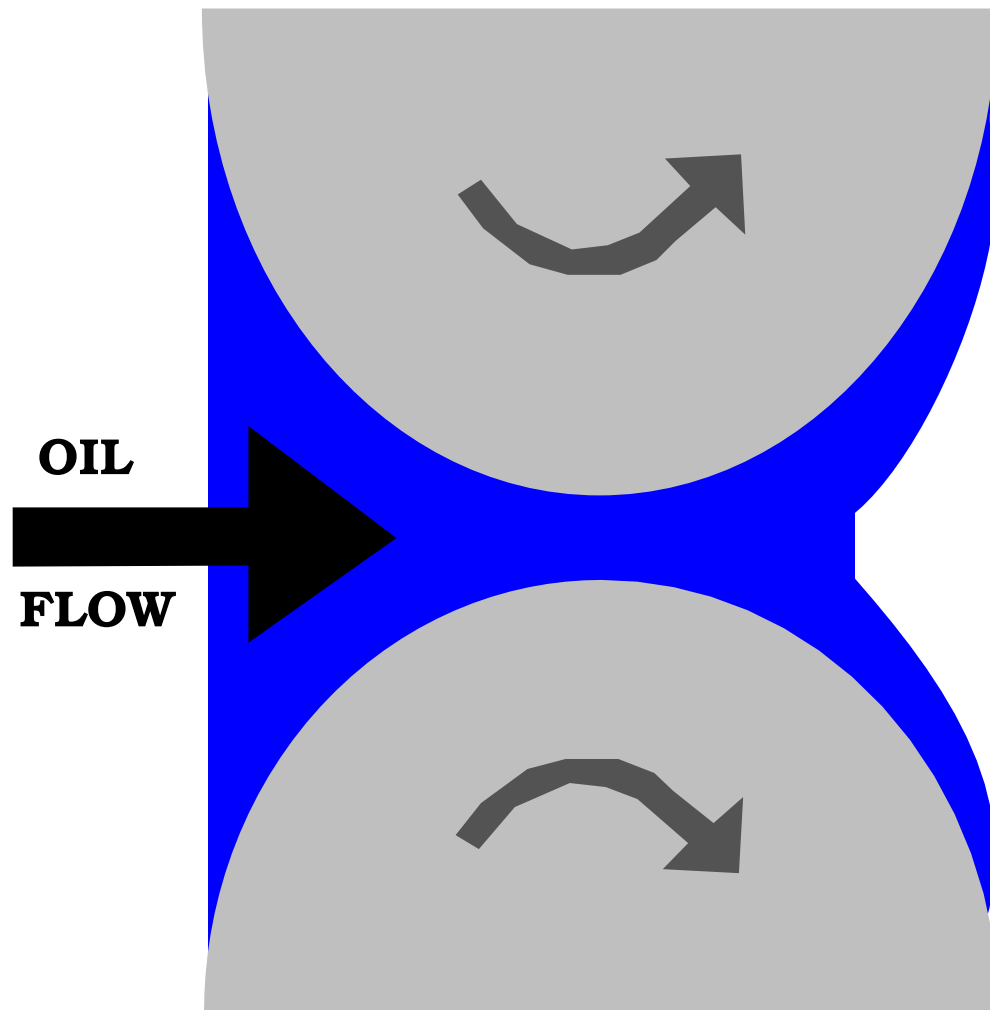
Chris Goodyer, Roger Fairlie, Martin Berzins

Thanks to Laurence Scales at Shell Global Solutions and Chris Taylor at Bradford!

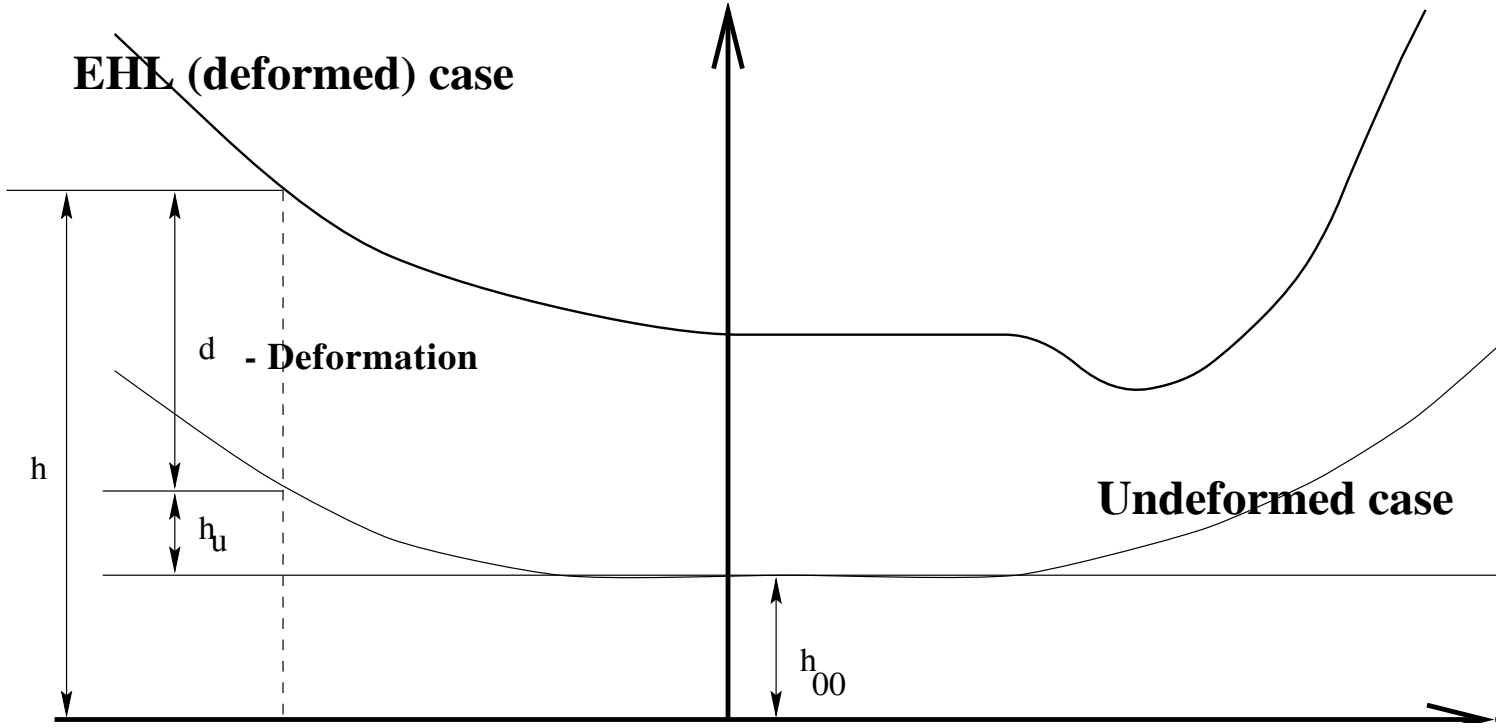
Talk outline

- What is elastohydrodynamic lubrication?
- Governing Equations
- The 1D line contact problem
 - Discretisation
 - Multilevel techniques
 - Example results
- The 2D circular contact problem
- Grid adaptation
- Solving transient problems
- PSEs
- Future work

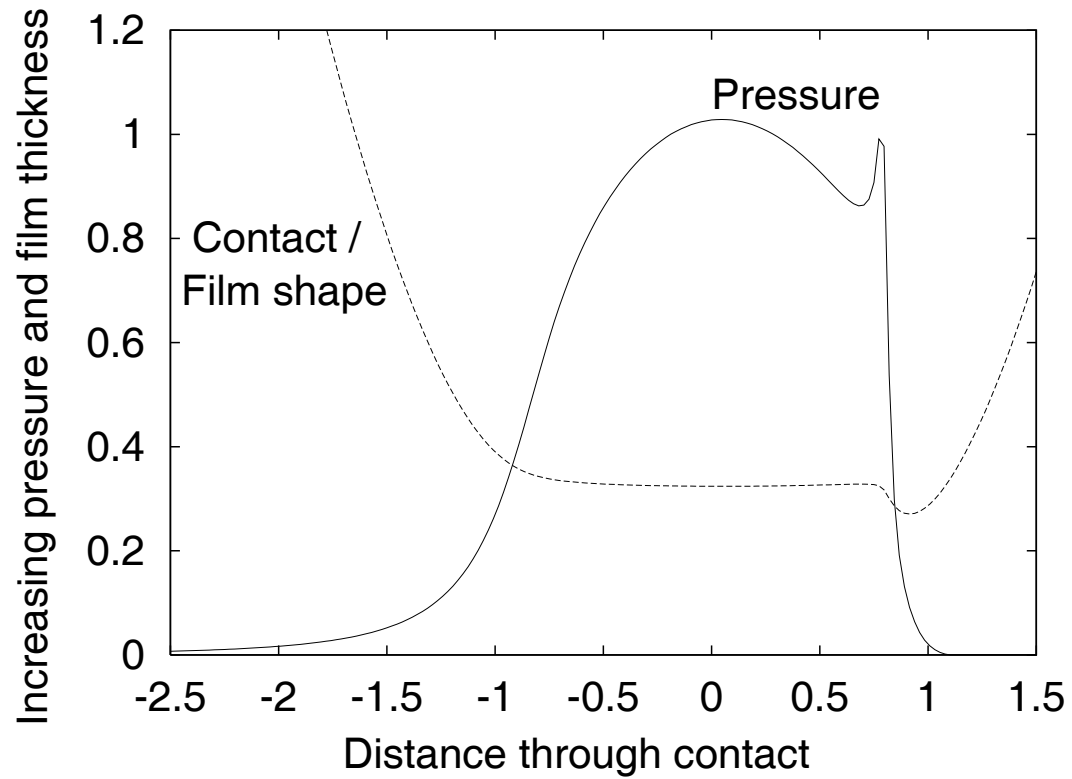
A hydrodynamic contact



(Elasto)hydrodynamic Lubrication Contacts



Geometry and Pressure plots across an EHL contact



Governing Equations I :

The Reynolds Equation

$$\frac{\partial}{\partial x} \left(\frac{\rho h^3}{\eta} \frac{\partial p}{\partial x} \right) + \frac{\partial}{\partial y} \left(\frac{\rho h^3}{\eta} \frac{\partial p}{\partial y} \right) = 6 \left\{ u_s \frac{\partial (\rho h)}{\partial x} + v_s \frac{\partial (\rho h)}{\partial y} + \rho h \frac{\partial u_s}{\partial x} + \rho h \frac{\partial v_s}{\partial y} + 2 \frac{\partial (\rho h)}{\partial t} \right\}$$

where,

p is the pressure, h is the film thickness, η is the viscosity,

ρ is the density, t is the time, x, y Cartesian coordinates

and u_s, v_s are the surface velocities in the x and y directions respectively.

Equation changes type in contact region.

Governing Equations II :

The Film Thickness Equation

1D line contact:

$$h(x, y) = h_{00} + \frac{x^2}{2R_x} + \frac{4}{\pi E'} \int_{-\infty}^{\infty} \ln \left| \frac{x - x'}{x_0} \right| p(x') dx'$$

2D circular point contact:

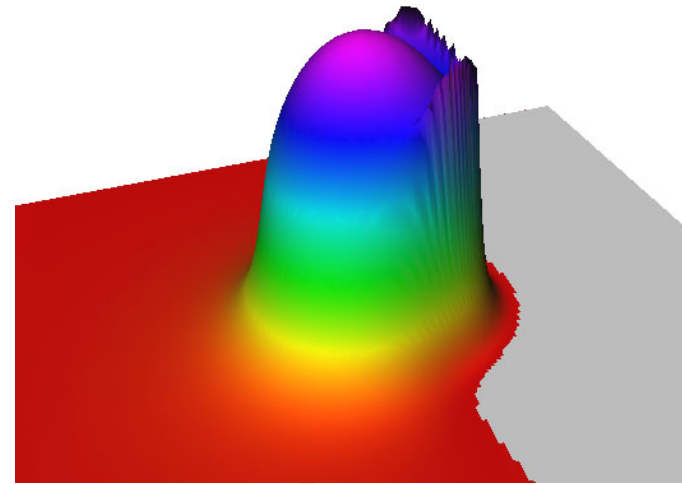
$$h(x, y) = h_{00} + \frac{x^2}{2R_x} + \frac{y^2}{2R_y} + \frac{2}{\pi E'} \int_{-\infty}^{\infty} \int_{-\infty}^{\infty} \frac{p(x', y') dx' dy'}{\sqrt{(x - x')^2 + (y - y')^2}},$$

Film thickness, h , at a point depends upon all the pressures!

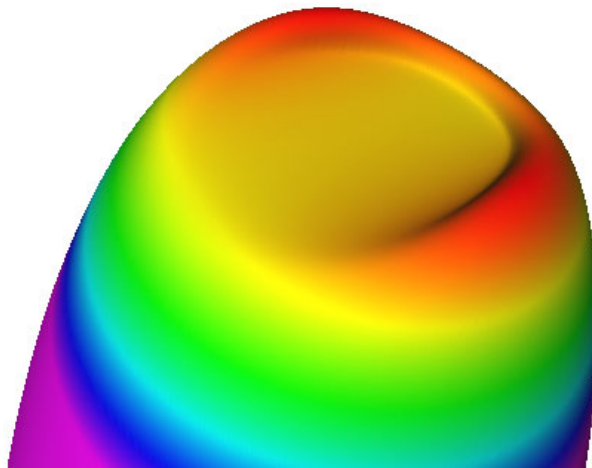
Conservation law - applied load carried entirely by lubricant film:

$$\int_{-\infty}^{\infty} \int_{-\infty}^{\infty} p(x, y) dx dy = F$$

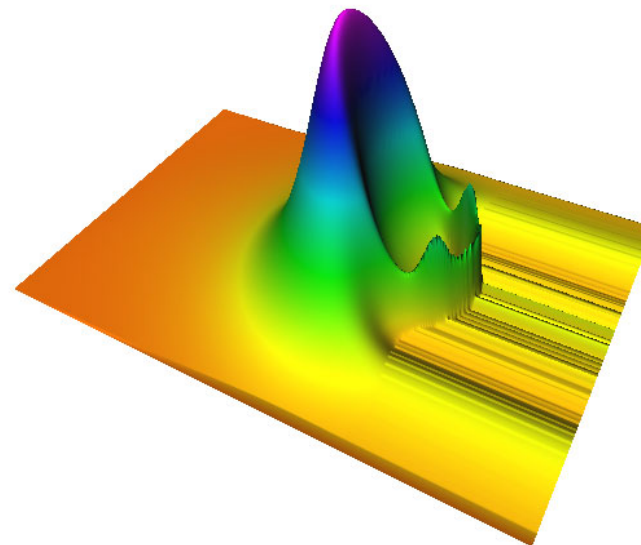
Typical solutions



Pressure



Film thickness



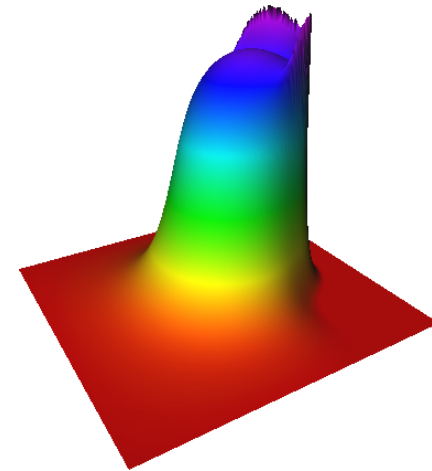
Temperature

Governing Equations III : Lubricant model (isothermal)

Density model: (Dowson and Higginson)

$$\rho(p) = \rho_0 \left(1 + \frac{5.8 \times 10^{-10} p}{1 + 1.7 \times 10^{-9} p} \right)$$

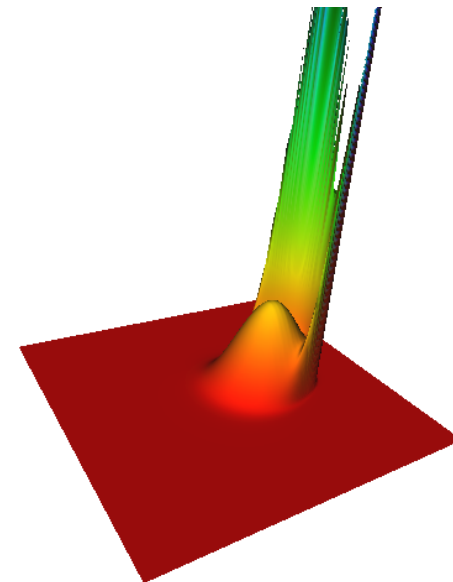
[Pictured non-dimensional range 1 → 1.16]



Viscosity Model: (from Roelands equation)

$$\eta(p) = \eta_0 \exp \left\{ \frac{\alpha p_0}{z} \left[-1 + \left(1 + \frac{p}{p_0} \right)^z \right] \right\}$$

[Pictured non-dimensional range 1 → 13300]



- More realistic rheological (non-Newtonian models) may be used instead

Governing Equations IV :

The Energy Equation

For thermal cases the Energy Equation also applies:

$$\rho \left\{ \frac{1}{2} \frac{\partial \theta}{\partial T} + U_m \frac{\partial \theta}{\partial X} + V_m \frac{\partial \theta}{\partial Y} + \frac{\theta - \theta_b}{H} \left[(U_m - U_b) \frac{\partial H}{\partial X} + V_m \frac{\partial H}{\partial Y} \right] \right\} =$$
$$\frac{3k}{2B^2 H^2} (\theta_a + \theta_b - 2\theta) + \beta_e \theta \left(\frac{1}{2} \frac{\partial P}{\partial T} + U_m \frac{\partial P}{\partial X} + V_m \frac{\partial P}{\partial Y} \right) -$$
$$2B\mu \left[\left(U_m - \frac{U_e}{2} \right) \frac{\partial P}{\partial X} - V_m \frac{\partial P}{\partial Y} \right] + \frac{B\mu\kappa}{3} \eta \Gamma_m^2$$

with the two surface temperatures given in the form

$$\theta_a(X) = 1 + 2\kappa\chi_a \int_{-\infty}^X \frac{(3\theta - 2\theta_a - \theta_b) d\zeta}{H(X) \sqrt{X - \zeta}}$$

Line Contact - Discretisation I

The Reynolds Equation:

$$\frac{1}{\Delta T} (\bar{\rho}_i H_i - \bar{\rho}_i^{t-1} H_i^{t-1}) = \frac{1}{\Delta X^2} \left(\varepsilon_{i+\frac{1}{2}} (P_{i+1} - P_i) - \varepsilon_{i-\frac{1}{2}} (P_i - P_{i-1}) \right) - \frac{1}{\Delta X} (\bar{\rho}_i H_i - \bar{\rho}_{i-1} H_{i-1})$$

where

$$\varepsilon_i = \frac{\bar{\rho}_i H_i^3}{\bar{\eta}_i \lambda}$$

The Film Thickness Equation:

$$H_i = H_{00} + X_i^2 - \frac{1}{\pi} \sum_{j=1}^n K_{ij} P_j$$

where $K_{ij} = (i - j + \frac{1}{2}) \Delta X (\ln(|i - j + \frac{1}{2}| \Delta X) - 1) - (i - j - \frac{1}{2}) \Delta X (\ln|i - j - \frac{1}{2}| \Delta X)$

The Force Balance Equation:

$$\Delta X \sum_{i=1}^n P_i = \frac{\pi}{2}$$

Line Contact - Discretisation II

The Density Equation:

$$\rho_i = \rho_0 \left(1 + \frac{\mu p_i}{1 + \nu p_i} \right) \{ 1 - \beta_e(p_i)(\theta_i - \theta_0) \}$$

where

$$\beta_e(p_i) = \beta_{e,0} \exp(-\kappa_e p_i)$$

The Viscosity Equation:

$$\eta = \eta_0 \exp \left(\frac{\alpha_0 p_0}{z_0} \left\{ \left(1 + \frac{p_i}{p_0} \right)^{z(\theta)} \left(\frac{\theta_i - \theta_r}{\theta_0 - \theta_r} \right)^{-s} - 1 \right\} \right)$$

where

$$z(\theta) = z_0 - z_1 \ln \left(\frac{\theta_i - \theta_r}{\theta_0 - \theta_r} \right)$$

and

$$s = \frac{\beta_0 z_0}{\alpha_0 p_0} (\theta_0 - \theta_r)$$

Line Contact - Discretisation III

The Energy Equation:

$$\bar{\rho}_i \left\{ \frac{(\theta_i^{t_n} - \theta_i^{t_{n-1}})}{2\Delta T} + U_m \frac{(\theta_i - \theta_{i-1})}{\Delta X} + \frac{(\theta_i - \theta_b)}{H} \left((U_m - U_b) \frac{H_i - H_{i-1}}{\Delta X} \right) \right\} =$$

$$\frac{3k}{2B^2 H_i^2} (\theta_a + \theta_b - 2\theta_i) + \beta_e \theta_i \left(\frac{(P_i^{t_n} - P_{i-1}^{t_{n-1}})}{2\Delta T} + U_m \frac{(P_i - P_{i-1})}{\Delta X} \right) -$$

$$2B\mu \left(U_m - \frac{U_e}{2} \right) \frac{(P_i - P_{i-1})}{\Delta X} + \frac{B\mu\kappa}{3} \eta_i \Gamma_m^2$$

where

$$U_m = -\frac{H_i^2}{2\kappa\eta_i} \frac{(P_i - P_{i-1})}{\Delta X} + \frac{U_e}{2}.$$

The Surface Temperature Equation:

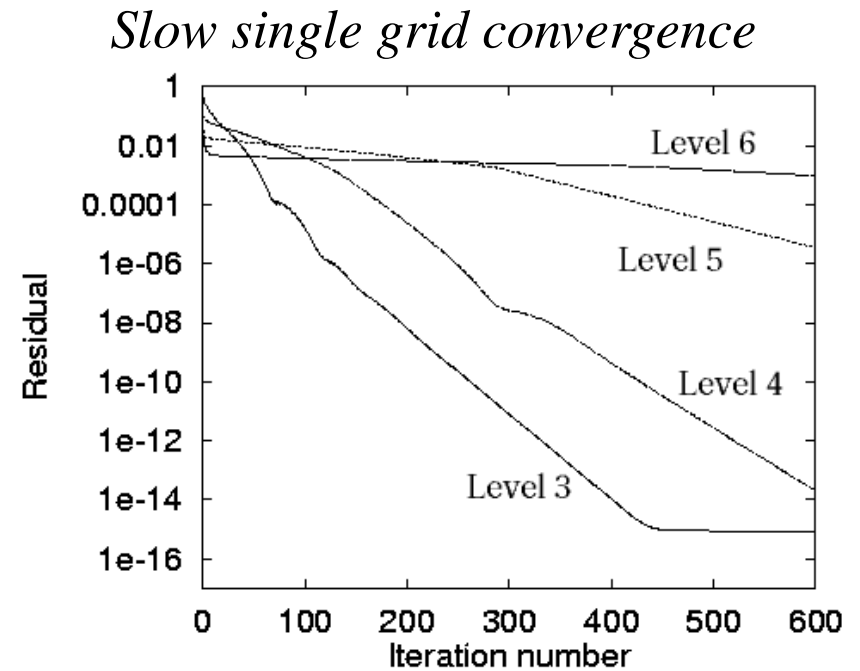
$$\theta_{a;i} = 1 + 4\kappa\chi_a \sum_{j=1}^i \left[\frac{\theta_{A;j-1} + \theta_{A;j}}{H_{j-1} + H_j} \left(\sqrt{X_j - X_{j-1}} - \sqrt{X_i - X_j} \right) \right]$$

Line Contact - Solution Methods

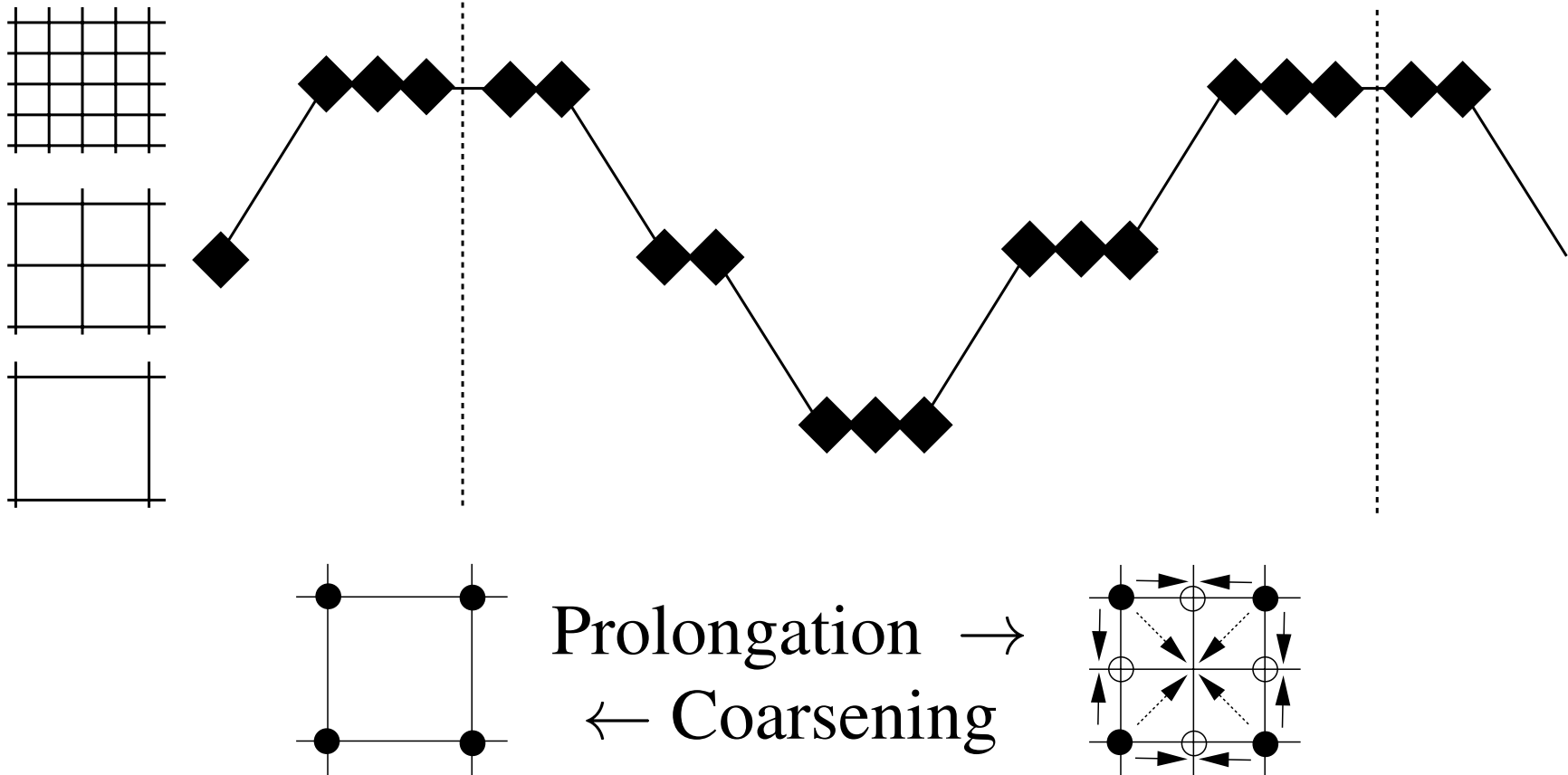
- Solve (non-linear) Reynolds equation for new Pressure
 - Use finite differences
 - Gauss-Seidel updates for whole line
 - Cavitation Region - Reynolds Equation not valid
- Update H using new P
 - Computationally expensive but Multi-level Multi-integration substantially reduces work
- Update Density and Viscosity
- Pointwise Jacobi scheme used to solve Energy Equation

Line Contact - Multigrid

- Standard iterative methods good at removing high frequency errors relative to grid
- Bad at removing low frequency errors relative to grid
- Use of multiple levels of grid refinement accelerate convergence on fine grids
- On fine meshes more of the errors are low frequency relative to grid

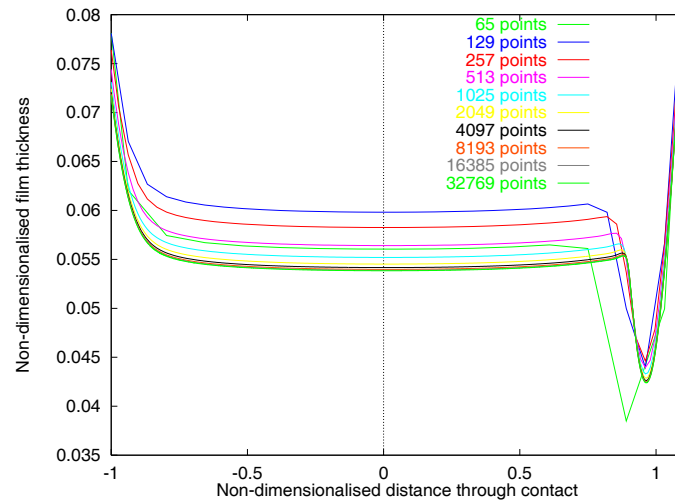
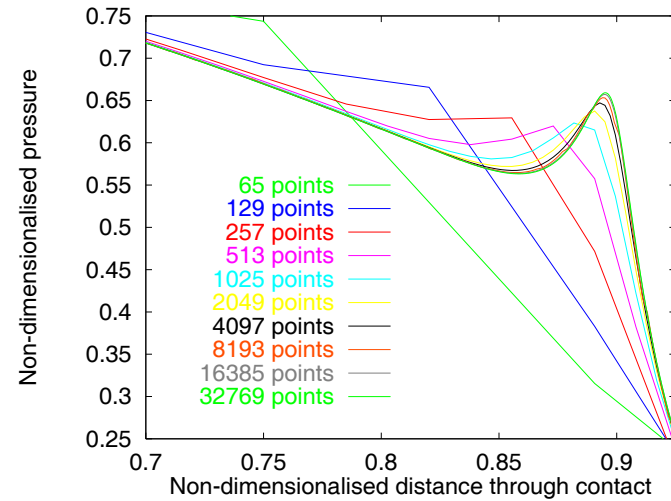
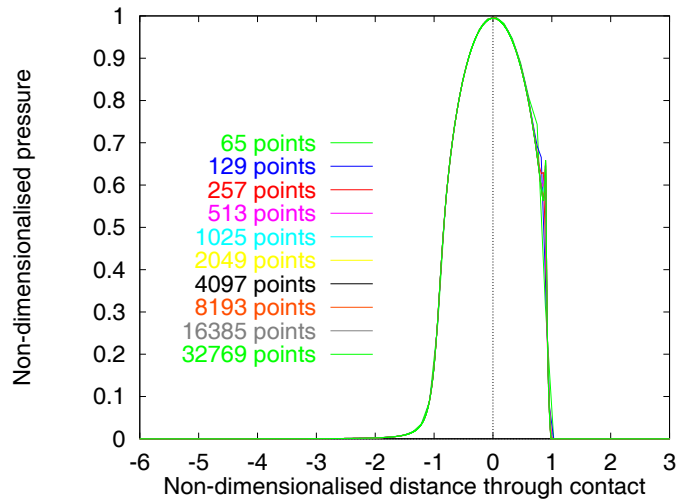


Multigrid Cycles



Adaptive multigrid may be used...

Line Contact - Pressure Spike Resolution

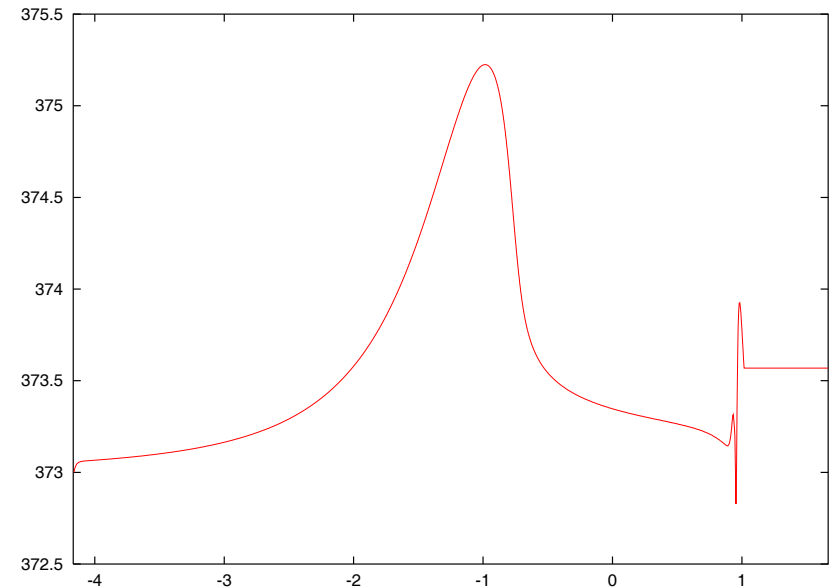


Line Contact - Thermal Effects

Thermal cases are important because there can be a significant temperature increase - up to 100° across the contact. This affects the friction in the contact.

The extent of these changes is governed by the type of lubricant being used, the fluid velocity and the slide to roll ratios.

Temperature across domain



Line Contact - Thermal Slide to Roll Ratios

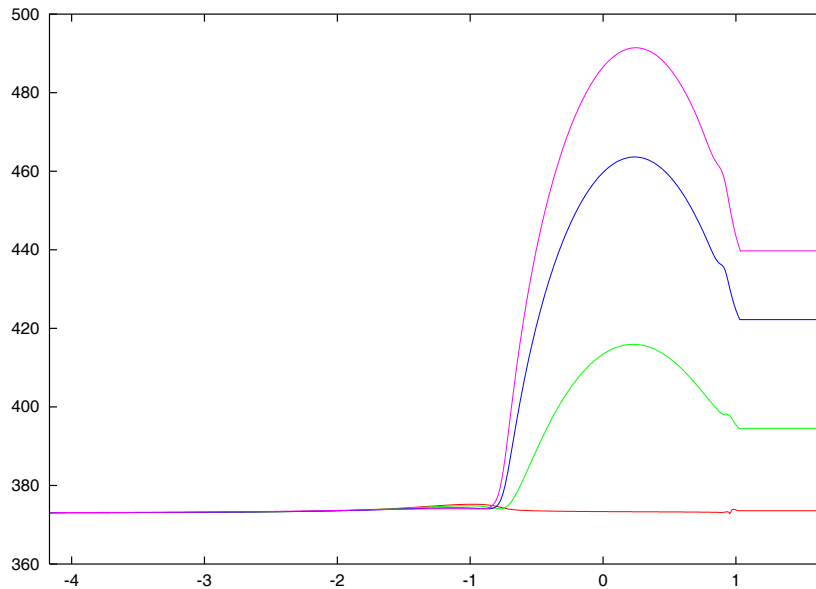
Slide to roll ratio given by

$$\mathcal{S} = \frac{2(u_2 - u_1)}{u_1 + u_2}$$

where u_1 and u_2 are the rolling velocities of the two surfaces.

Shown is the same example as the previous slide with pure rolling ($\mathcal{S}=0$) in red, with increasing shear ($\mathcal{S} = 0.34, 1, 1.4$).

Temperature across domain



Line Contact - Thermal Surface Features Movies

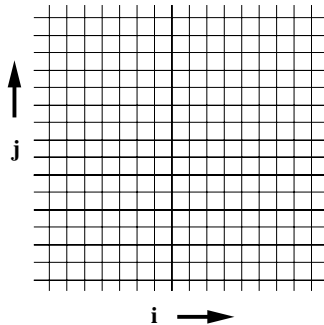
Point Contact - Discretisation I

The Reynolds Equation:

$$\begin{aligned} \frac{1}{\Delta T} (\bar{\rho}_{i,j} H_{i,j} - \bar{\rho}_{i,j}^{t-1} H_{i,j}^{t-1}) &= \frac{1}{\Delta X^2} \left[\varepsilon_{i+\frac{1}{2},j} (P_{i+1,j} - P_{i,j}) - \varepsilon_{i-\frac{1}{2},j} (P_{i,j} - P_{i-1,j}) \right] \\ &+ \frac{1}{\Delta Y^2} \left[\varepsilon_{i,j+\frac{1}{2}} (P_{i,j+1} - P_{i,j}) - \varepsilon_{i,j-\frac{1}{2}} (P_{i,j} - P_{i,j-1}) \right] \\ &- \frac{1}{\Delta X} (\bar{\rho}_{i,j} H_{i,j} - \bar{\rho}_{i-1,j} H_{i-1,j}) \end{aligned}$$

where

$$\varepsilon_{i,j} = \frac{\bar{\rho}_{i,j} H_{i,j}^3}{\bar{\eta}_{i,j} \bar{\lambda}}$$



The Force Balance Equation:

$$\Delta X \Delta Y \sum_{i=1}^{N_X} \sum_{j=1}^{N_Y} P_{i,j} = \frac{2\pi}{3}$$

Point Contact - Discretisation II

The Film Thickness Equation:

$$H_{i,j} = H_{00} + \frac{X_i^2}{2} + \frac{Y_j^2}{2} - \frac{2}{\pi^2} \sum_{k=1}^{N_X} \sum_{l=1}^{N_Y} K_{i,j,k,l} P_{k,l}$$

where $K_{i,j,k,l} = \frac{2}{\pi^2} \left\{ \begin{aligned} &|X_p| \sinh^{-1} \left(\frac{Y_p}{X_p} \right) + |Y_p| \sinh^{-1} \left(\frac{X_p}{Y_p} \right) \\ &- |X_m| \sinh^{-1} \left(\frac{Y_p}{X_m} \right) - |Y_p| \sinh^{-1} \left(\frac{X_m}{Y_p} \right) \\ &- |X_p| \sinh^{-1} \left(\frac{Y_m}{X_p} \right) - |Y_m| \sinh^{-1} \left(\frac{X_p}{Y_m} \right) \\ &+ |X_m| \sinh^{-1} \left(\frac{Y_m}{X_m} \right) + |Y_m| \sinh^{-1} \left(\frac{X_m}{Y_m} \right) \end{aligned} \right\}$

Point Contact - Discretisation III

The Energy Equation:

$$\begin{aligned} \bar{\rho}_i & \left\{ \frac{\theta_{i,j} - \theta_{i,j}^{t_{n-1}}}{2\Delta T} + U_m \frac{\theta_{i,j} - \theta_{i-1,j}}{\Delta X} + \frac{\theta_{i,j} - \theta_b}{H_{i,j}} \left[(U_m - U_b) \frac{H_{i,j} - H_{i-1,j}}{\Delta X} + V_m \frac{H_{i,j} - H_{i,j-1}}{\Delta Y} \right] \right\} \\ & = \frac{3k}{2B^2 H_{i,j}^2} (\theta_a + \theta_b - 2\theta_{i,j}) + \beta_e \theta_{i,j} \left[\frac{P_{i,j} - P_{i-1,j}^{t_{n-1}}}{2\Delta T} + U_m \frac{P_{i,j} - P_{i-1,j}}{\Delta X} + V_m \frac{P_{i,j} - P_{i,j-1}}{\Delta Y} \right] - \\ & \quad 2B\mu \left[\left(U_m - \frac{U_e}{2} \right) \frac{P_{i,j} - P_{i-1,j}}{\Delta X} - V_m \frac{P_{i,j} - P_{i,j-1}}{\Delta Y} \right] + \frac{B\mu\kappa}{3} \eta_{i,j} \Gamma_m^2 \end{aligned}$$

where $U_m = -\frac{H_{i,j}^2}{2\kappa\eta_{i,j}} \frac{P_{i,j} - P_{i,j-1}}{\Delta X} + \frac{U_e}{2}$ and $V_m = \frac{H_{i,j}^2}{2\kappa\eta_{i,j}} \frac{P_{i,j} - P_{i,j-1}}{\Delta Y}$

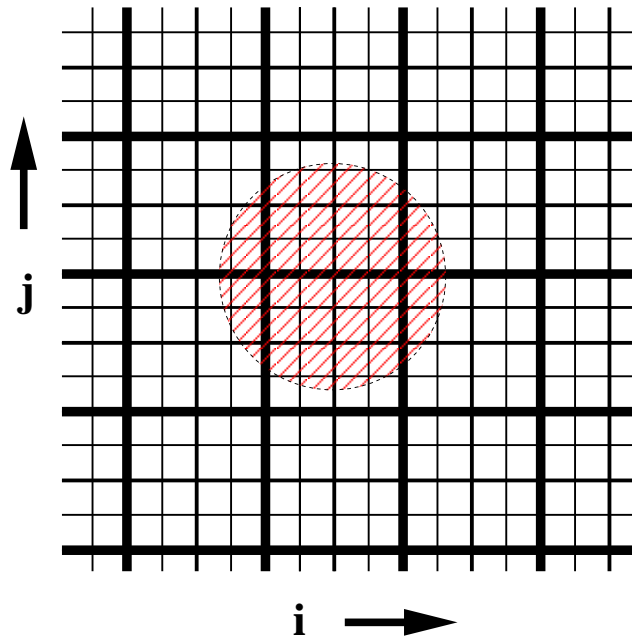
The Surface Temperature Equation:

$$\theta_{a;i,j} = 1 + 4\kappa\chi_a \sum_{k=1}^i \left[\frac{\theta_{A;k-1,j} + \theta_{A;k,j}}{H_{k-1,j} + H_{k,j}} \left(\sqrt{X_k - X_{k-1}} - \sqrt{X_i - X_k} \right) \right]$$

Point Contact - Solution methods

- Solve (non-linear) Reynolds equation for new Pressure
 - Contact Region solution schemes include:
 - * Distributive scheme [Lubrecht & Venner]
 - * Jacobi Line [Nurgat & Berzins]
 - Non-contact region - G-S Line scheme
 - Cavitation Region - Reynolds Equation not valid
- Update H using new P
 - Computationally expensive but Multilevel Multi-integration substantially reduces work
- Update Density and Viscosity
- Evaluate Energy Equation by pointwise Jacobi along each line

Line Contact - Multilevel Multi-Integration



- Aim is to reduce work by summing over as few elements as possible
- Sum over fine grid points near singularity
- Add sum from all coarse grid points
- Correct in region of influence

$$H_{i,j} = H_{00} + \frac{X_i^2}{2} + \frac{Y_j^2}{2} - \frac{2}{\pi^2} \sum_{k=1}^{N_X} \sum_{l=1}^{N_Y} K_{i,j,k,l} P_{k,l}$$

This is similar to the fast multipole method

Point Contact - MLMI Speed-ups

MLMI computational times (s) for a single film thickness calculation

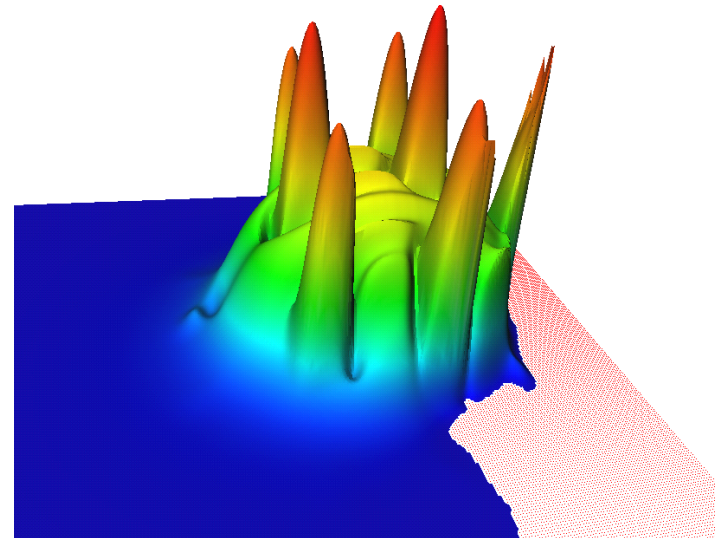
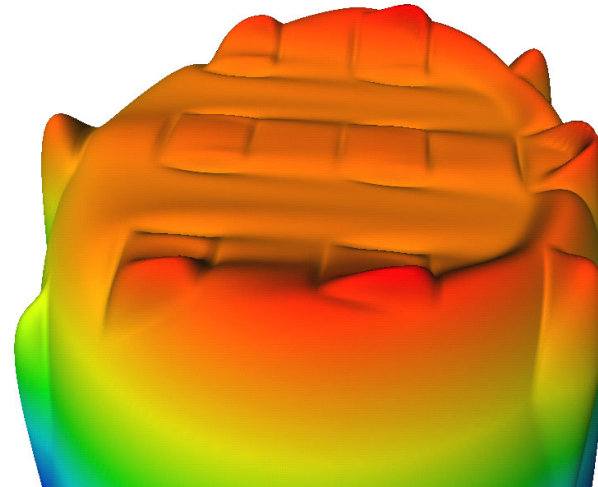
		Coarsest grid used in multi-integration				
		Level 3	Level 4	Level 5	Level 6	Level 7
Level	5	0.14	0.22	2.29	-	-
of	6	0.35	0.50	2.30	28.5	-
solution	7	1.14	1.26	3.21	28.2	397

Root mean square error of a typical calculation

		Level 3	Level 4	Level 5	Level 6
Level	5	3.2×10^{-5}	1.2×10^{-5}	-	-
of	6	3.5×10^{-5}	1.8×10^{-5}	7.2×10^{-6}	-
solution	7	3.7×10^{-5}	2.1×10^{-5}	1.0×10^{-5}	3.8×10^{-6}

Surface Roughness

- Real surfaces are not smooth
- Surface geometry can now be measured
- Detail requires very fine meshes - hence fast solvers
- Important in fields where gap is very narrow
- Many roughness problems *transient*

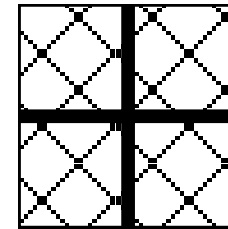
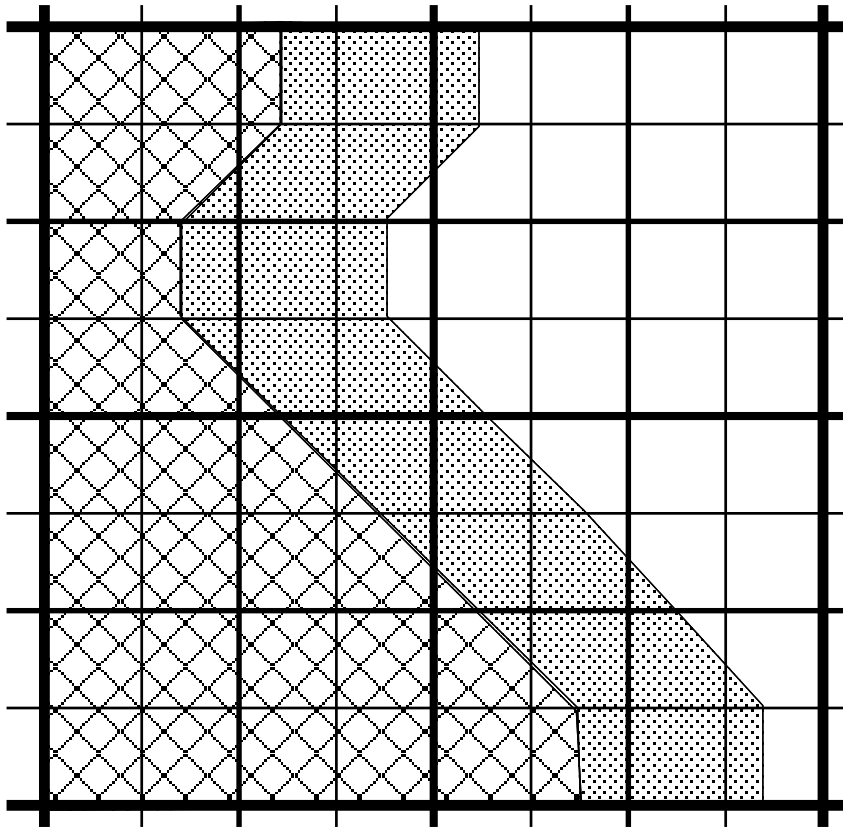


Grid Adaptation

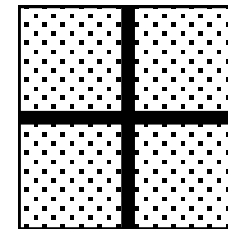
- EHL calculations are very expensive on fine meshes
- Interesting behaviour restricted to the contact area
- Inlet region very important for good solutions
- Adaptive meshing allows solutions of similar accuracy, but cheaper
- Refine based on either:
 - pre-defined geometry
 - monitor function, e.g. pressure
 - Error test
- Work concentrated where needed

Deformation calculation not yet done on an adapted mesh

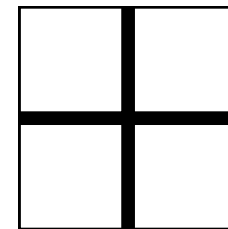
Grid Adaptation - Free boundary treatment



Pressure positive
point



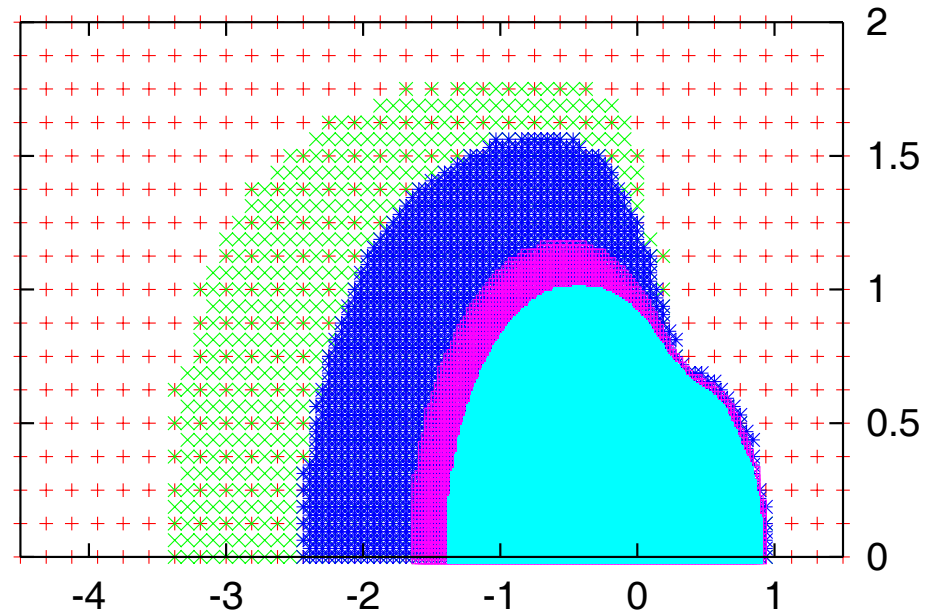
Cavitation point
included in
adaptive solve



Cavitation point
excluded from
adaptive solve

At least one point inside the cavitation region (zero pressure) included in each pressure solve

Grid Adaptation - Results



Grid dimension	Adaptation style	Speed up
129×129	Geometry	37.7%
257×257	Monitor function	49.9%
513×513	Error test	48.8%

Differential Algebraic Formulation

In discretised form, for solution vectors \underline{P} , \underline{H} and $\underline{\rho}$, the system can be written:

$$\text{Reynolds Equation: } \underline{F}(\underline{P}, \underline{\rho H}, [\underline{\rho \dot{H}}]) = 0$$

$$\text{Film thickness: } \underline{H} = \underline{h_0} + K\underline{P}$$

K is a large dense block Toeplitz (non-singular?) matrix

There is no explicit transient derivative of pressure, hence this is not an ODE but a DAE system

Assuming non-singularity this has DAE index 1

Transient EHL Problems

- EHL is an inherently transient field
- Novel use of a standard ODE solver coupled with standard convergence test linked to MG solver
- Continue iterations to reduce errors using Shampine convergence test:

$$\frac{\sigma}{1 - \sigma} \left\| \underline{H}^{(m+1)}(t_n) - \underline{H}^{(m)}(t_n) \right\| < 0.33tol$$

where tol is an error tolerance for the iteration, $\| \cdot \|$ a suitable norm, m the multigrid iteration number, and σ is an estimate of the rate of convergence

- Use of standard ODE techniques to predict next timestep solutions

Variable Time Stepping using Local Error Control

- Define the local errors in \underline{H} and \underline{P} by \underline{leH} and \underline{leP}
- Standard error equations in DAE form [Petzold]

$$\begin{bmatrix} -1 - \Delta T \frac{\partial \underline{F}_1}{\partial \underline{\rho H}} & -\Delta T \frac{\partial \underline{F}_1}{\partial \underline{P}} \\ -\Delta T & \Delta T K \end{bmatrix} \begin{bmatrix} \underline{leH} \\ \underline{leP} \end{bmatrix} = \begin{bmatrix} -1 & 0 \\ 0 & 0 \end{bmatrix} \frac{1}{2} \begin{bmatrix} H_n - H_n^{pred} \\ P_n - P_n^{pred} \end{bmatrix}$$

- This gives $\underline{leH} = K \underline{leP}$ and the standard estimate for the local error:

$$-\Delta T \left(\frac{\underline{leH}}{\Delta T} + \frac{\partial \underline{F}_1}{\partial \underline{\rho H}} \underline{leH} + \frac{\partial \underline{F}_1}{\partial \underline{P}} \underline{leP} \right) = -\frac{(H_n - H_n^{pred})}{2}$$

- Assume zero residuals and applying Taylor's Theorem:

$$\underline{E}_1 \left(\underline{\tilde{P}}, \underline{\tilde{\rho}\tilde{H}_n}, [\underline{\tilde{\rho}\dot{\tilde{H}}_n}] \right) = \frac{(H_n - H_n^{pred})}{2\Delta T}$$

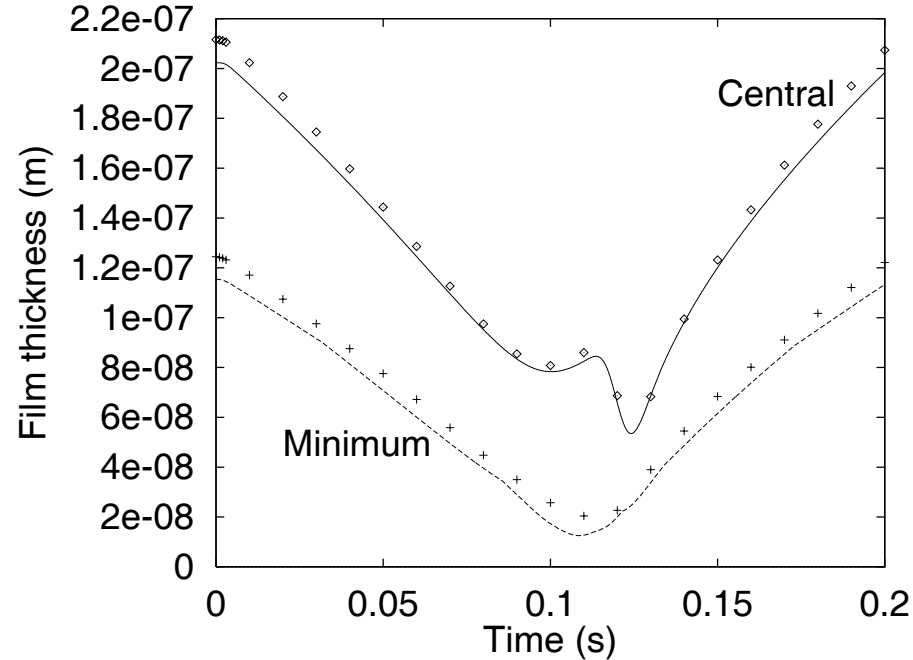
- Solve using multigrid to estimate $\|\underline{leH}\|_\omega = \|\underline{\tilde{H}}_{n+1} - \underline{H}_{n+1}\|_\omega$
- Same equation systems as before, but different RHS
- Only use \underline{H} rather than \underline{H} & \underline{P} in error convergence test
- Choose TOL to represent spatial error:

$$ATOL = \frac{1}{10} \sqrt{\frac{1}{N_x^C N_y^C} \sum_{I=1}^{N_x^C} \sum_{J=1}^{N_y^C} [\tilde{H}_{i,j} - \tilde{H}_{I,J}]^2}$$

- Stepsize ratio, $r = (2 \|\underline{leH}\|_\omega)^{\frac{-1}{k+1}}$
- Contrast with standard EHL $\Delta T = \Delta X$ fixed step method

Transient EHL Problem - Reversal

- Models mechanical situations where engine parts move, eg cams, gears
- Entrainment velocity slows down • Goes through 0ms^{-1} at 0.1s
- Speeds up in opposite direction

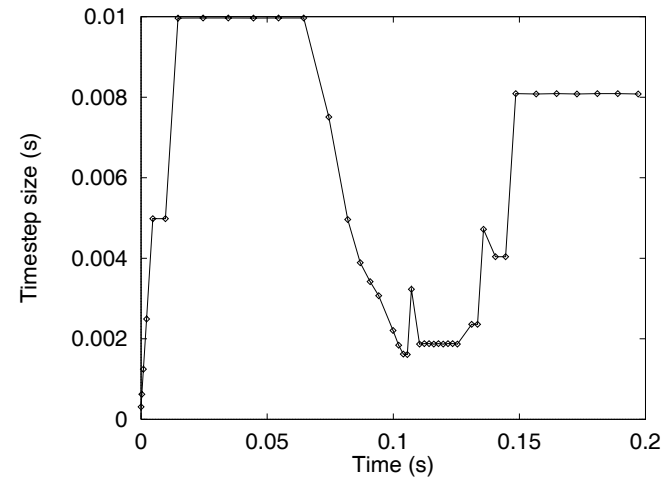
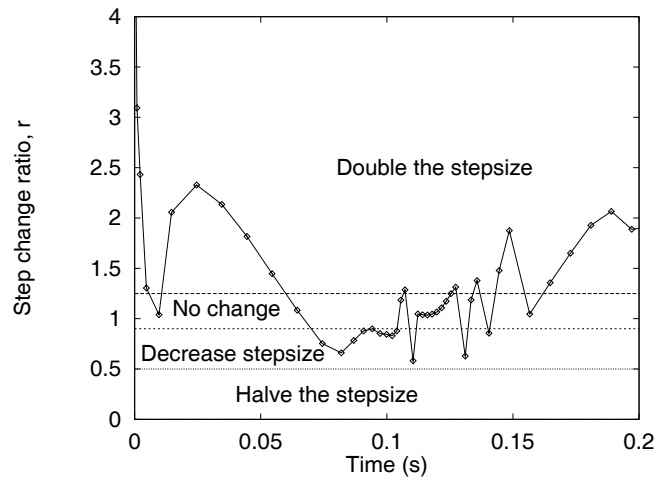
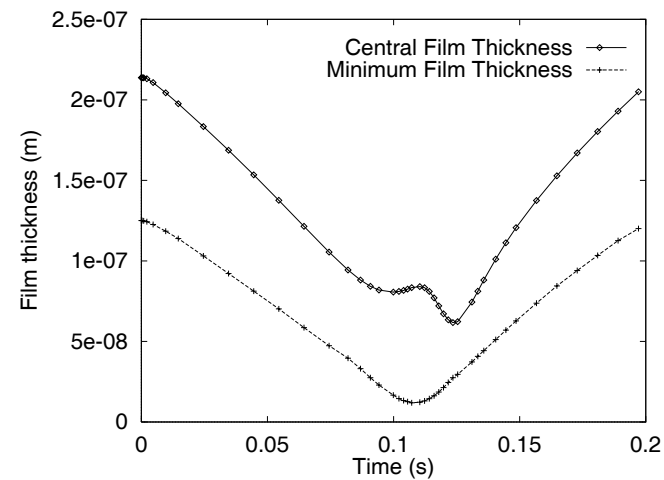


Plot of central and minimum film thickness

Transient EHL Problem - Reversal

Reversal from 0.05ms^{-1} to -0.05ms^{-1} in 0.2s.

Variable Time Stepping in Action



Problem Solving Environments (PSEs)

PSEs are advantageous because they

- allow synchronous computation and visualisation
- can connect powerful visualisation tools to every dataset
- remove the need for much recompilation of codes
- allow users to change the problem being solved mid-stream

Dataflow often through a pipeline structure joining together modules for different tasks.

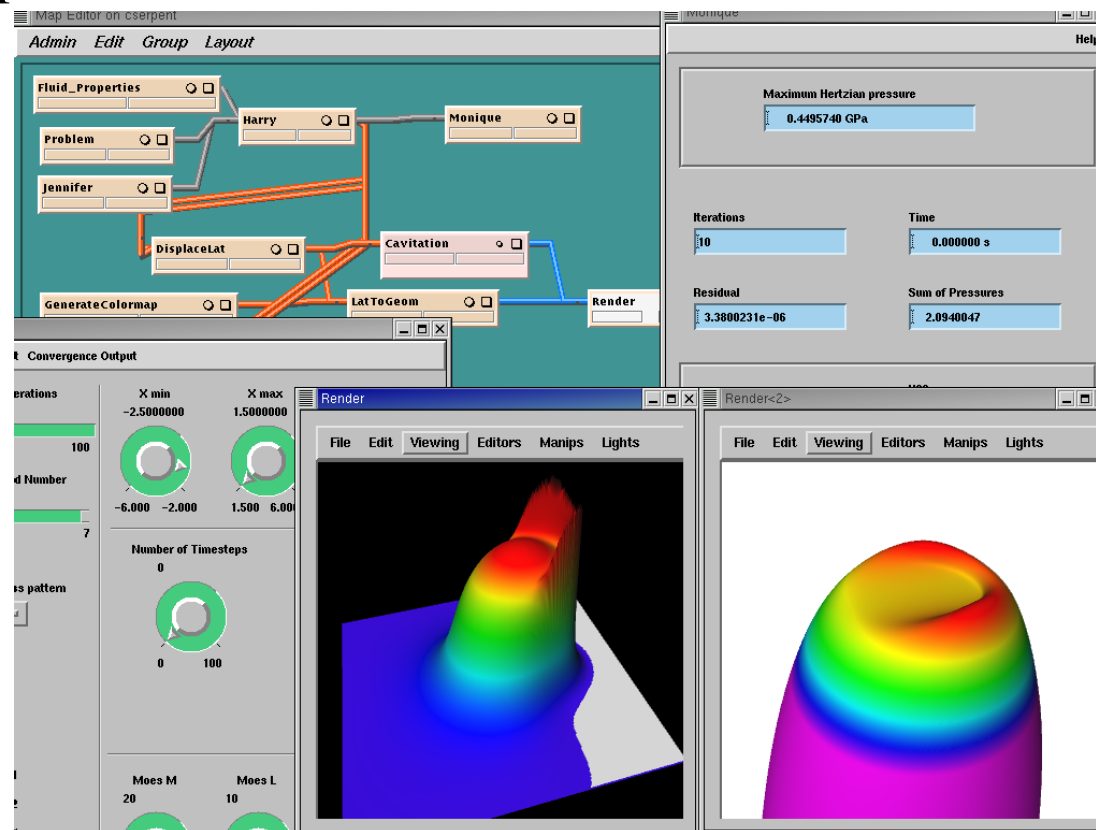
PSEs - Module Control Panel

The screenshot displays the PSEs Module Control Panel with various control elements and annotations:

- Level of Output** and **Convergence Output** are displayed at the top.
- Iterations:** A slider for **Max Iterations** is set to 10, with a range from 1 to 100.
- Grid level:** A slider for **Max Grid Number** is set to 7, with a range from 3 to 7.
- Surface features:** The **Roughness pattern** is set to **Ridge**. The **X-offset** is set to 0.0000000, with a range from -2.500 to 1.500.
- Relaxation parameters:** A dropdown menu is set to 0.2, with options 0.1, 0.2, and 0.4.
- Steering capabilities:** **Run** and **Initialise** buttons are visible.
- Domain size:** Three circular gauges for **X min** (-2.5000000), **X max** (1.5000000), and **Ymax** (2.0000000). Below them are gauges for **X** (-6.000 to -2.000) and **Y** (1.500 to 6.000).
- Transient options:** **Number of Timesteps** is set to 6, and **Timestep Size** is set to 0.001000000. Below are gauges for **X** (0 to 100) and **Y** (1.000e-05 to 0.1000). A **Transient case** dropdown is set to **Surface features**.
- Non-dimensional parameters:** Three circular gauges for **Moes M** (35), **Moes L** (10), and **Material G** (4700.0000). Below them are gauges for **X** (5 to 100), **Y** (5 to 50), and **Z** (1000. to 7000.).

PSEs - ECLIPSE in IRIS Explorer

IRIS Explorer is a commercial “visual programming environment for customised visualisation applications” – NAG.



PSEs - ELLIPSE in SCIRun

SCIRun has been developed by the University of Utah and is a computational workbench for visual programming.

- Again operates on a pipeline structure
- It is a multi-threaded package - hence ease of parallelisation
- Modules may be rewired mid-firing thanks to the threads
- It is completely open source

Future Work

- More adaptive meshing
- Transient rheological models
- More detailed (realistic?) surface features
- Development of parallelism tools available for use